Biology of Reproduction, 2018, 98(5), 695–704
doi:10.1093/biolre/ioy006
Research Article
Advance Access Publication Date: 17 January 2018

Research Article

Effects of excess thromboxane A_2 on placental development and nutrient transporters in a *Mus musculus* model of fetal growth restriction†

Karen J. Gibbins[1,*], Katherine N. Gibson-Corley[2], Ashley S. Brown[3], Matthew Wieben[3], Richard C. Law[3] and Camille M. Fung[3]

[1]Division of Maternal-Fetal Medicine, Department of Obstetrics and Gynecology, University of Utah, Salt Lake City, Utah, USA; [2]Department of Pathology, University of Iowa, Iowa City, Iowa, USA and [3]Division of Neonatology, Pediatrics, University of Utah, Salt Lake City, Utah, USA

*__Correspondence__: Division of Maternal-Fetal Medicine, Department of Obstetrics & Gynecology, University of Utah, 50 N Medical Drive, Salt Lake City, Utah 84132, USA. Email: kgibbins@hsc.utah.edu

†__Grant Support:__ KJG received support from the University of Utah WRHR program 1K12HD085816 NICHD.
__Conference Presentation:__ Presented in part at the 2016 Pediatric Academic Societies annual meeting, 30 April-3 May, 2016, Baltimore, Maryland.

Received 14 June 2017; Revised 22 November 2017; Accepted 16 January 2018

ABSTRACT

Hypertensive disease of pregnancy (HDP) with placental insufficiency is the most common cause of fetal growth restriction (FGR) in the developed world. Despite the known negative consequences of HDP both to the mother and fetus, little is known about the longitudinal placental changes that occur as HDP progresses in pregnancy. This is because longitudinal sampling of human placentae during each gestation is impossible. Therefore, using a mouse model of thromboxane A_2-analog infusion to mimic human HDP in the last trimester, we calculated placental efficiencies based on fetal and placental weights; quantified spongiotrophoblast and labyrinth thicknesses and vascular density within these layers; examined whether hypoxia signaling pathway involving vascular endothelial growth factor A (VEGFA) and its receptors (VEGFR1, VEGFR2) and matrix metalloproteinases (MMPs) contributed to vascular change; and examined nutrient transporter abundance including glucose transporters 1 and 3 (GLUT1, GLUT3), neutral amino acid transporters 1, 2, and 4 (SNAT1, SNAT2, and SNAT4), fatty acid transporters 2 and 4 (FATP2, FATP4), and fatty acid translocase (CD36) from embryonic day 15.5 to 19 in a 20-day C57Bl/6J mouse gestation. We conclude that early-to-mid gestation hypertensive placentae show compensatory mechanisms to preserve fetal growth by increasing placental efficiencies and maintaining abundance of important nutrient transporters. As placental vascular network diminishes over late hypertension, placental efficiency diminishes and fetal growth fails. Neither hypoxia signaling pathway nor MMPs mediated the vascular diminution in this model. Hypertensive placentae surprisingly exhibit a sex-differential expression of nutrient transporters in late gestation despite showing fetal growth failure in both sexes.

Summary Sentence

Excess thromboxane A_2 leads to a mouse phenotype of hypertensive disease of pregnancy and fetal growth restriction with evidence of altered placental vascular development and nutrient transporter abundance.

Key words: placenta, placental transport, preeclampsia, intrauterine growth restriction, angiogenesis.

Introduction

Fetal growth restriction (FGR) affects 5%–10% of human pregnancies in developed countries depending on the criteria used. Etiologies of FGR can be of maternal, placental, or fetal origin such as maternal medical conditions, maternal substance use and teratogens, fetal genetic disorders, infectious diseases, multiple gestation, and placental pathologies [1]. Placental insufficiency is the most common etiology of FGR in the developed world and is associated with significant short- and long-term morbidities [2]. Placental insufficiency occurs when a placenta fails to deliver adequate oxygen and nutrients to the developing fetus. Both maternal and fetal adaptive mechanisms typically activate to attempt to sustain fetal growth, but when these adaptive mechanisms fail, FGR results, and in the most extreme cases results in stillbirth [3].

Multiple human placental studies have evaluated the histopathologic findings associated with placental insufficiency-mediated FGR. These findings include abnormal trophoblast invasion, decreased placental perfusion, and abnormal fetal angiogenesis [4–7]. Of note, placental vascular lesions are commonly found in severe FGR and are also found in preeclampsia, particularly in early-onset pre-eclampsia [8, 9]. None of these lesions however are pathognomonic for placental insufficiency-mediated FGR; they merely describe the state of the placentae at the end of gestation without any information about the processes culminating in FGR.

In order to understand the dynamic placental changes that occur during the development of placental insufficiency and FGR, we have chosen to use a well-established mouse model of FGR that has been shown to duplicate many features of the human FGR phenotype [10–12]. Using this model, we can sample placentae longitudinally during the mouse gestation to gain first-hand information about the developmental and adaptive changes within the FGR placentae. The mouse placenta is an appropriate model system to interrogate human disease due to its similar structure and function as the human placenta. Both human and mouse placentae are hemochorial meaning that fetally derived trophoblast tissue is directly bathed in maternal blood. The murine chorioallantoic placenta is evident by embryonic day (*E*) 10.5–11.5 in a 20-day gestation when the hemisection along the sagittal plane reveals four histologically distinct layers [13]. Located furthest from the fetus is the maternal decidua. Abutting the decidua is the parietal trophoblast giant cell layer that overlies the spongiotrophoblast layer. Together this is named the junctional zone. The labyrinth layer, situated below the junctional zone, is analogous to human chorionic villi [14]. The labyrinth layer contains two separate convoluted and highly branched vascular networks—one fetal and one maternal, tortuously intertwined for optimal nutrient, gas, and waste exchange. In addition, both the murine labyrinth layer and the human chorionic villi share similar diffusion capacities, enzyme and transport activities critical for fetal nutrient accretion.

As previously mentioned, FGR is most commonly due to placental insufficiency in developed countries. Thromboxane A_2 (TXA_2), a potent vasoconstrictor and platelet aggregator that normally acts in balance with the vasodilator prostacyclin in human pregnancy, is abnormally elevated in many etiologies of FGR, such as hypertensive disease of pregnancy (HDP), diabetes mellitus, and tobacco smoking [15, 16]. Thus, using a mouse model of FGR based on diseases with TXA_2 overproduction is logical. In this model, we have previously shown that dams exposed to U-46619 (a TXA_2 analog) have mean blood pressure that is elevated by 20% and that mouse pups showed 15% decreases in both brain weight and body weight compared to pups born from sham surgery [10].

The aims of this current study were twofold. We first hypothesized that the underlying etiology of placental insufficiency and FGR in this mouse model was due to maldevelopment of the placental vasculature. We explored whether an aberrant hypoxia signaling pathway or aberrant matrix metalloproteinases (MMPs) would be associated with placental vascular maldevelopment. For the hypoxia signaling pathway, we examined the protein abundance of hypoxia-inducible factor 1α (HIF-1α), hypoxia-inducible factor 2α (HIF-2α), hypoxia-inducible factor 1β (HIF-1β = ARNT), Egl-9 family hypoxia inducible factor 1 (PHD2), Von Hippel-Lindau tumor suppressor (VHL), and vascular endothelial growth factor A (VEGFA) and its vascular endothelial growth receptor 1 and 2 (VEGFR1 and VEGFR2). For MMPs, we examined the protein abundance of gelatinases (MMP2 and MMP9), membrane-type MMPs (MMP14, MMP15, MMP16, MMP17, MMP24, MMP25), and extracellular matrix metalloproteinase inducer (EMMPRIN = CD147). We additionally hypothesized that these hypertensive placentae would exhibit early compensatory mechanisms to preserve placental and fetal growth but ultimately exhibit placental growth failure culminating in fetal growth failure. We focused on measuring placental and fetal growth and determining the protein abundance and localization of important nutrient transporters such as glucose transporters GLUT1 and GLUT3, neutral amino acid transporters SNAT1, SNAT2, and SNAT4, as well as fatty acid transporters FATP2 and FATP4, and fatty acid translocase CD36 throughout the last week of mouse gestation when maternal hypertension was evident and fetal growth was most restricted.

Materials and methods

Mouse model of HDP via maternal thromboxane A_2 (TXA_2) analog (U-46619) infusion

All procedures were approved by the University of Utah Animal Care committee and carried out in accordance with NIH Guide for the Care and Use of Laboratory Animals. Maternal hypertension was induced according to Fung et al. [10]. Briefly, timed matings of C57BL/6J mice (stock#000664, The Jackson Laboratory, Bar Harbor, ME) were set up. At embryonic day (*E*) *12.5*, pregnant dams were anesthetized and micro-osmotic pumps (product#1007D, Durect Corporation, Cupertino, CA) containing either vehicle (0.5% ethanol = sham group) or U-46619 (a TXA_2 analog, product#16450, Cayman Chemical, Ann Arbor, MI, at 4000 ng/μl, dissolved in 0.5% ethanol, and infused at 0.5 μl/h) were implanted into dams for the remainder of pregnancy (term gestation ~20 days). Previous model characterization had shown that maternal mean blood pressures of dams receiving U-46619 infusion were elevated by 20% by the second day of pump implantation. At *E*15.5, *E*17.5, and *E*19, dams were re-anesthetized for caesarean sections and pups and placentae were obtained. We recorded all pup and placenta weights.

Histological examination of the developing placentae at E15.5, E17.5, and E19 using hematoxylin and eosin stain

Harvested sham and hypertensive placentae at *E*15.5, *E*17.5, and *E*19 were immersed and fixed in 10% neutral buffered formalin

for 24 h at room temperature. After fixation, placentae were dehydrated through a series of graded ethanol baths and then embedded in paraffin wax. Five-micrometer thick sections were cut with a microtome and mounted onto microscope slides. Routine hematoxylin and eosin stain was used to examine placental histopathology. We quantified the thicknesses of the spongiotrophoblast and labyrinth layers under ×2 magnification (n = 4–8/group) using an Olympus BX53 microscope. Photomicrographs were taken with an Olympus DP72 camera, and each layer was outlined manually with Olympus Cell Sens software for quantification.

Immunohistochemical CD31, VEGFR1, and VEGFR2 staining of the developing placentae at E15.5, E17.5, and E19

All mounted sections first underwent antigen retrieval with Tris EDTA, pH 9.0 at 125°C for 5 min in a decloaker for CD31 and with citrate buffer, pH 6.0 at 110°C for 20 min in a decloaker for VEGFR immunohistochemistry. Endogenous peroxidase activity was quenched with 3% hydrogen peroxide. We blocked nonspecific sites with either 10% horse serum (CD31) or 5% horse serum (VEGFR1 and VEGFR2). Sections were then incubated with monoclonal rat anti-CD31 (prod#550274, BD Pharmingen, San Jose, CA, one section each from n = 3–6/group) at 1:25 overnight at 4°C, monoclonal rabbit anti-VEGFR1(prod#NB110–57643, Novus Biologicals, Littleton, CO, one section each from n = 6/group) at 1:250 for 60 min at room temperature, or monoclonal rabbit anti-VEGFR2 (prod#2479, Cell Signaling, Boston, MA, one section each from n = 6/group) at 1:850 overnight at 4°C (see full list of antibodies under Supplementary Table S1). Slides were then incubated with the appropriate secondary antibody and detection was visualized using biotinylated anti-rat or rabbit IgG at 1:200 followed by ABC (Vectastain Elite, Vector Laboratories, Burlingame, CA) for CD31 or DAKO Rabbit Envision HRP System reagent for 30 min for VEGFR1 and VEGFR2. Slides were then developed with DAKO DAB plus for 5 min followed by DAB Enhancer for 3 min before being counterstained with hematoxylin. Tissues were examined with an Olympus BX53 microscope. CD31, VEGFR1, and VEGFR2 immunostaining were quantified using Aperio whole-slide scanning technology and a color deconvolution algorithm to determine the percentage of positive immunostaining of the whole placenta.

Western immunoblotting for the abundance of placental hypoxia signaling proteins HIF-1α, HIF-2α, HIF-1β, PHD2, VHL, and VEGFA, and matrix metalloproteinases 2, 9, 14, 15, 16, 17, 24, 25, and EMMPRIN (CD147) at E19 and of placental glucose transporters GLUT1 and GLUT3, neutral amino acid transporters SNAT1, SNAT2, and SNAT4, and fatty acid transporters FATP2, FATP4, and fatty acid translocase CD36 at E15.5, E17.5, and E19

Harvested placentae at the various gestational ages were initially flash-frozen and stored at –80°C prior to analyses. Ground placentae were first homogenized in ice-cold RIPA buffer to extract membrane proteins (n = 6/group, one male and one female from six separate litters in each experimental group). We separated 20 μg of proteins on 4%–12% Bis-Tris gels by XT Criterion gel electrophoresis (product#345–0123, Bio-Rad Laboratories, Hercules, CA) at 160 V for 75 min. We transferred proteins to polyvinylidene fluoride membranes (Millipore, Billerica, MA) for 1 h at RT and blocked membranes in 5% milk/Tris-buffered saline Tween (TBS-T) for 1 h at RT. We incubated membranes with the following antibodies: HIF-1α (prod#PA116601, ThermoFisher Scientific, Waltham, MA) at 1:200, HIF1β (prod#PA316508, ThermoFisher Scientific) at 1:200, HIF2α (prod#PA116510, ThermoFisher Scientific) at 1:300, PHD2 (prod#PA116524, ThermoFisher Scientific) at 1:300, VHL (prod#PA527322, ThermoFisher Scientific) at 1:200, VEGFA (prod#PA516754, ThermoFisher Scientific) at 1:100, MMP2 (prod#PA516504, ThermoFisher Scientific) at 1:200, MMP9 (prod#PA513199, ThermoFisher Scientific) at 1:200, MMP14 (prod#PA516514, ThermoFisher Scientific) at 1:100, MMP15 (prod#PA513184, ThermoFisher Scientific) at 1:400, MMP16 (prod#PA528966, ThermoFisher Scientific) at 1:400, MMP17 (prod#PA528219, ThermoFisher Scientific) at 1:200, MMP24 (prod#PA551333, ThermoFisher Scientific) at 1:100, MMP25 (prod#PA513191, ThermoFisher Scientific) at 1:100, CD147 (prod#11989–1-AP, Proteintech) at 1:100; GLUT1 (prod#07–1401, Millipore) at 1:500, GLUT3 (prod#ab41525, Abcam, Cambridge, MA) at 1:500, SNAT1 (prod#PA542420, ThermoFisher Scientific) at 1:500, SNAT2 (prod#SC-67081, Santa Cruz Biotech, Santa Cruz, CA) at 1:400, SNAT4 (prod#SC-67085, Santa Cruz Biotech) at 1:200, FATP2 (prod#ab175373, Abcam) at 1:200, FATP4 (prod#ab199719, Abcam) at 1:500, and CD36 (prod#ab133625, Abcam) at 1:500 for 1 h at RT (see full list of antibodies under Supplementary Table S1). We detected protein abundance with a horseradish peroxidase-conjugated anti-rabbit secondary antibody or horseradish peroxidase-conjugated anti-rat secondary antibody at 1:10,000 for 1 h at RT, developed with Western Lighting enhanced chemiluminescence (prod#NEL104001, PerkinElmer, Waltham, MA), and quantified with Image Lab (Bio-Rad Laboratories). We used GAPDH at 1:5000 (prod#2118, Cell Signaling) or α-tubulin at 1:5000 (prod#62204, ThermoFisher Scientific) as our loading controls as the expression of these housekeeping genes is unaltered in this model.

Immunofluorescent staining of SNAT1, SNAT2, SNAT4, FATP2, and FATP4 at E19

Paraffin-embedded sections cut at 5 μm and mounted on slides were used (one section each from n = 4/group). We first melted the paraffin at 75°C for 1 h in an oven. We then placed slides into Histoclear II (prod#64111–01, Electron Microscopy Sciences, Hatfield, PA) for 10 min three times, followed by 100% ethanol for 3 min three times, 95% ethanol for 3 min, 70% ethanol for 3 min, and deionized water for 3 min three times. We pursued antigen retrieval with either universal antigen retrieval reagent (prod#CTS015, R&D Systems, Minneapolis, MN) for SNAT4 or basic antigen retrieval reagent (prod#CTS013, R&D Systems) for the rest at 95°C for 15 min. After washing with deionized water, we blocked sections with either 10% normal mouse serum or goat serum for 2 h. We used the following primary antibodies: SNAT1 (prod#MABN502, Millipore) at 1:100, SNAT2 (prod#SC-67081, Santa Cruz) at 1:200, SNAT4 (prod#SC-67085, Santa Cruz) at 1:100, FATP2 (prod#ab83763, Abcam) at 1:100, and FATP4 (prod#ab199719, Abcam) at 1:100 (see full list of antibodies under Supplementary Table S1). We detected protein localization with 1:2000–1:2500 goat anti-mouse or anti-rabbit secondary antibody conjugated with Alexa 488 for all nutrient transporters. TO-PRO-3 stain (prod#T3605, ThermoFisher Scientific) was used for nuclei counterstaining. Sections were viewed with an Olympus Fluoview FV1000 confocal microscope under ×20 and ×40 oil immersion lenses (NA 0.80 and

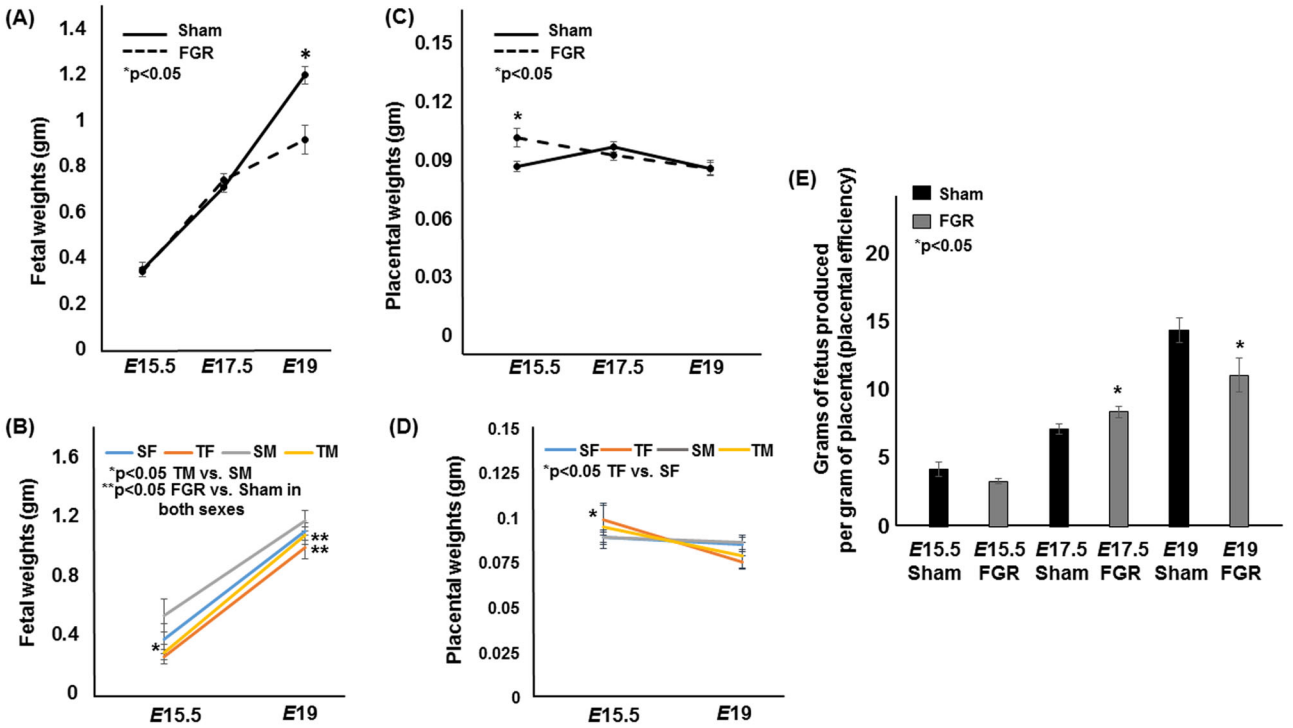

Figure 1. Fetal weights, placental weights, and placental efficiencies of sham and TXA_2 analog exposed (FGR) pregnancies at *E*15.5, *E*17.5, and *E*19. (A) The solid line denotes sham fetal weights, while the dotted line denotes FGR fetal weights. (B) Fetal weights at *E*15.5 and *E*19 separated out by sex. (C) The solid line denotes sham placental weights, while the dotted line denotes FGR placental weights. (D) Placental weights at *E*15.5 and *E*19 separated by sex. (E) Placental efficiencies defined as grams of fetus produced per gram of placenta of sham and FGR gestations. *Statistical significance declared at $P < 0.05$.

0.85, respectively) and imaged with the Fluoview software (version 4.2). Negative controls omitting primary antibodies were used to subtract background fluorescence.

Statistics

Pup and placenta weights and placental efficiencies were denoted as means ± SEM. We calculated the placental labyrinth-to-spongiotrophoblast thickness ratios and CD31, VEGFR1, and VEGFR2 labyrinth-to-spongiotrophoblast ratios and denoted them as means ± SEM. We expressed western blot data as means ± SEM based on the ratios of the abundance of the protein of interest and GAPDH or α-tubulin. We ensured that all data were tested for normality and equal variances before parametric tests were used. We analyzed all means with one-way ANOVA between sham and FGR groups of both sexes at each gestational age and used two-way ANOVA to detect differences between sexes and treatment groups at each gestational age. Statistical significance was declared at $P < 0.05$ using the STATVIEW software (Cary, NC).

Results

Fetal and placental weights and placental efficiencies across gestation

We have previously shown that fetal weights diverged between sham and FGR pups by *E*19 [10]. Our current cohort of mouse pups replicated the previous finding that FGR pups were growth restricted at *E*19 (Figure 1A). Additionally, we found that *E*15.5 FGR male pups weighed less than *E*15.5 sham male pups (n = 12 for sham and n = 15 for FGR, Figure 1B). Intriguingly, placentae from hypertensive pregnancies weighed more at *E*15.5 which was driven higher by FGR female placentae (n = 12 for sham and n = 15 for FGR, Figure 1C and D). The trajectory of the hypertensive placental growth however diminished over gestation (n = 14 and 28 for sham at *E*17.5 and *E*19 respectively and n = 21 and 19 for FGR at *E*17.5 and *E*19 respectively) whereas sham-operated dams had similar placental weights from *E*15.5 to *E*19 (Figure 1C and D). When we examined placental efficiencies defined as grams of fetus produced per gram of placenta, it was increased at *E*17.5 (Figure 1E). But at *E*19, we saw a significant decrease in placental efficiency, likely driven by the fetus' inability to gain weight at this age despite a placental weight that is similar to the sham placenta. We also noted no difference in litter sizes between sham and FGR pregnancies similar to our previous report (6.3 ± 0.3 in sham vs. 6.4 ± 0.5 in FGR, $P > 0.05$) [10].

Development of labyrinth and spongiotrophoblast layers across gestation

The labyrinth-to-spongiotrophoblast thickness ratios were similar between sham and hypertensive placentae showing that the gross architecture of the hypertensive placenta was intact (n = 6/group/gestational age, Figure 2A). When we examined CD31 (PECAM-1) staining, the vasculature in both *E*17.5 and *E*19 hypertensive placentae was significantly decreased in the labyrinth layer and this decrease was progressive over time (n = 6/group/gestational age, Figure 2B). To elucidate a potential mechanism for decreased vasculature in *E*17.5 and *E*19 hypertensive placentae, we examined the abundance of VEGFR1 and VEGFR2. Both receptors bind to VEGF but VEGFR1 is anti-angiogenic compared to VEGFR2

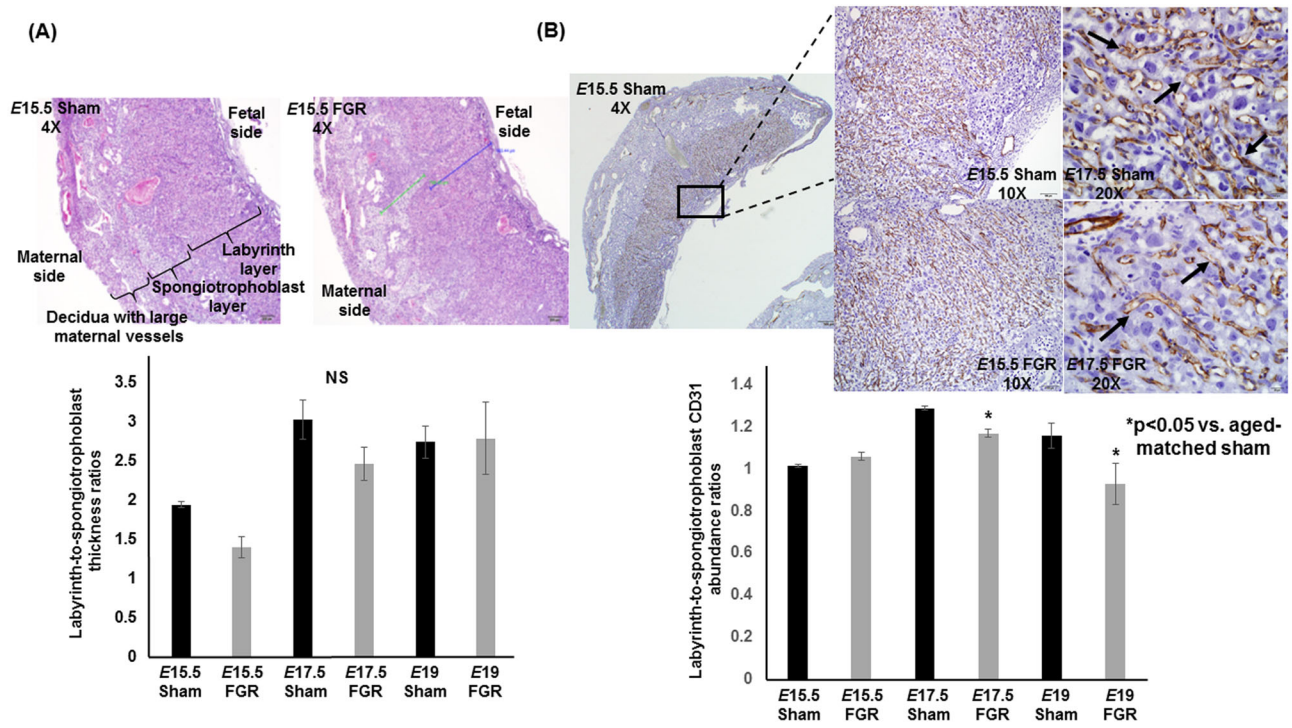

Figure 2. Labyrinth-to-spongiotrophoblast thickness ratios and labyrinth-to-spongioblast CD31 abundance ratios of sham and TXA_2 analog exposed (FGR) murine placentae at *E*15.5, *E*17.5, and *E*19. (A) Photomicrographs of representative hematoxylin and eosin cross sections at ×4 magnification of sham and FGR placentae at *E*15.5 above. Quantification of labyrinth-to-spongiotrophoblast thickness ratios depicted in the graph below. The blue line and green line in FGR placenta depict the actual measurements of labyrinth layer and spongiotrophoblast layer, respectively. NS denotes no statistical significance between sham and FGR placentae at any age. (B) Photomicrographs of representative CD31 immunostaining cross sections at ×4, ×10, and ×20 magnification of sham and FGR placentae at *E*15.5 and *E*17.5 above. Quantification of labyrinth-to-spongiotrophoblast CD31 abundance ratios depicted in the graph below. *Statistical significance declared at $P < 0.05$ for age-matched sham.

which is pro-angiogenic. We found no differences in either VEGFR abundance at either time point between sham and FGR placentae (n = 6/group/gestational age, data not shown). When we examined whether the abundance of hypoxia signaling pathway proteins or MMPs could explain the decreased vasculature in FGR placentae at *E*19, we detected no differences in either proteins between sex-matched sham and FGR placentae, i.e. no difference between sham females vs. FGR females or between sham males vs. FGR males (Figure 3A and B, Supplementary Figures S1 and S2). However, significant sex differences exist across all four groups. For example, HIF-1α and HIF-2α in sham males and FGR males were consistently lower in abundance than FGR females (*c* and *d* in Figure 3A). Similar observations were made with MMPs showing significant sex differences across all four groups but no differences when comparing sham females to FGR females or sham males to FGR males.

Nutrient transporter abundance and localization across gestation

At *E*15.5, hypertensive placentae had increased FATP4 and CD36 abundance while other transporters had similar expression compared to sham placentae (n = 6/group, Figure 4A). At *E*17.5, we detected no differences in any transporter abundance showing that all transporters were equal in expression between sham and FGR placentae (n = 6/group, data not shown). Given the significant growth failure evident at *E*19 coupled with the known differential catch-up growth rate between FGR males and females in postnatal life in this model, we examined placental transporter abundance with an additional variable of the fetal sex that the placenta supported. Intriguingly, FGR decreased the abundance of neutral amino acid transporter SNAT1 only in placentae supporting female pups (Figure 4B), whereas FGR increased the abundance of neutral amino acid transporters SNAT1, SNAT2, and SNAT4 as well as fatty acid transporters FATP2 and FATP4 in placentae supporting male pups (n = 6/group, Figure 5). Localization with immunofluorescent staining showed that these nutrient transporters were localized to the fetal trophoblastic cells within the labyrinth layer rather than in fetal endothelial cells (Figure 6).

Discussion

In a mouse model of FGR that mimics human pregnancies complicated by TXA_2 overproduction such as in HDP, we demonstrated that the placenta during early-to-mid hypertension is capable of mounting compensatory mechanisms to sustain fetal growth by increasing placental efficiency. However, placental efficiency ultimately diminishes in late gestation when fetal demands increase exponentially prior to delivery. We additionally demonstrated that placental labyrinth vasculature reduction is a prominent feature of mid-to-late FGR placentae in this model, suggesting that placental vascular insufficiency is a reason for FGR. Mechanistically, labyrinth vasculature reduction was neither associated with a change in the hypoxia signaling pathway nor in the MMPs that degrade and remodel specific components of the extracellular matrix for trophoblast and vascular invasion. To maintain fetal growth in early hypertension,

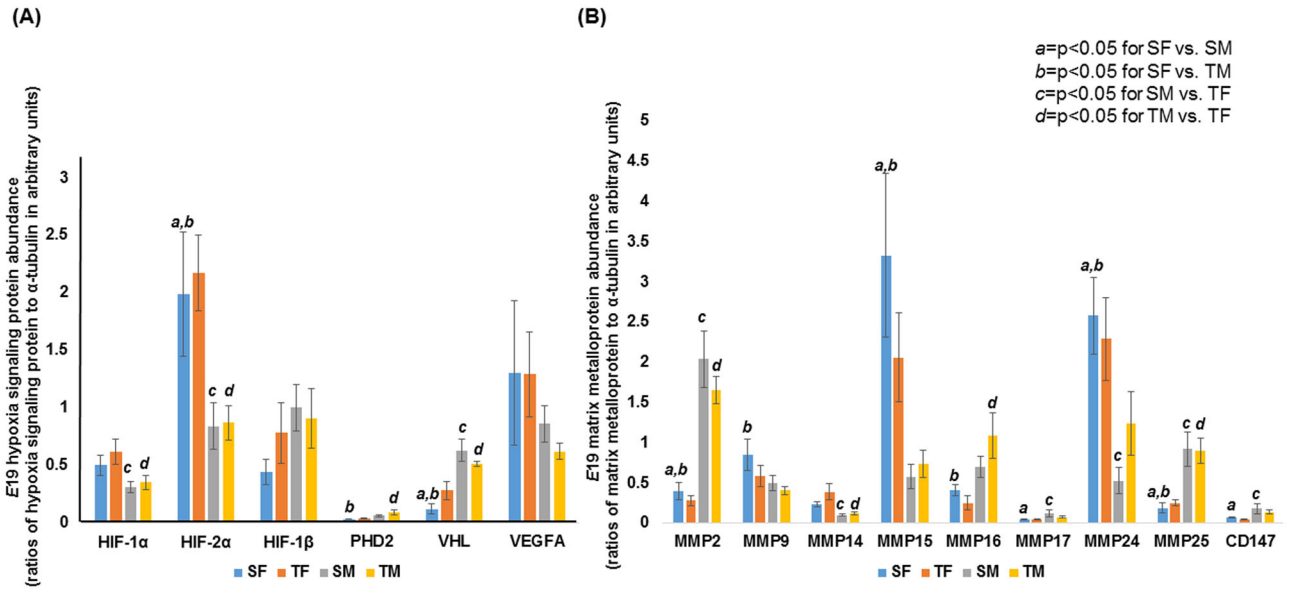

Figure 3. Western blot data of *E*19 hypoxia signaling proteins and matrix metalloproteinases of sham and TXA*2* analog exposed (FGR) placentae separated out by sex. (A) Quantification of HIF-1α, HIF-2α, HIF-1β, PHD2, VHL, and VEGFA protein abundance is depicted. (B) Quantification of gelatinases (MMP2, MMP9), membrane-type MMPs (MMP14, MMP15, MMP16, MMP17, MMP24, MMP25), and EMMPRIN (CD147) is depicted. *a* denotes statistical significance between sham females (SF) and sham males (SM) at $P < 0.05$. *b* denotes statistical significance between sham females (SF) and TXA_2 analog exposed males (TM) at $P < 0.05$. *c* denotes statistical significance between sham males (SM) and TXA_2 analog exposed females (TF) at $P < 0.05$. *d* denotes statistical significance between TXA_2 analog exposed females (TF) and TXA_2 analog exposed males (TM) at $P < 0.05$.

increasing transporter for fatty acids appears to be the preferred substrate. However, as hypertension continues toward the end of gestation, we found that depending on the fetal sex that the placenta supports, placental abundance of important nutrient transporters is differentially expressed. FGR female placentae show a decrease in neutral amino acid transporter whereas FGR male placentae show increased neutral amino acid and fatty acid transporter (FATP).

The implications of our findings are many. The major determinant of fetal growth in mammals is the placental supply of nutrients to the fetus [17], which occurs primarily by diffusion and transporter-mediated transport [18]. In turn, these processes depend upon the size, morphology, blood flow, and transporter abundance of the placenta. In our model, sham-operated pups gain weight steadily while placental weights remain similar over the last week of gestation. On the contrary, FGR males weighed lighter than sham males at early hypertension with both sexes showing a slower rate of rise in weight by *E*19. Intriguingly, FGR female placentae weighed the most during early hypertension, potentially showing better adaptation to sustain FGR female growth over FGR male growth. We additionally observed an increase in placental efficiency in mid-hypertension which diminished in late gestation. Increased placental efficiency could signify enhanced transplacental transfer of nutrients per gram of placenta. Conversely, large placentae appear to be less efficient irrespective of whether overgrowth is produced genetically or by environmental manipulations early in development [19]. Our increase in placental insufficiency likely represents enhanced transplacental transfer of nutrients during early hypertension as FATP4 and CD36 are upregulated and fetal growth is sustained. However, FGR placental weights ultimately show a downward trajectory over time such that in late hypertension, poor placental growth is mirrored with poor fetal growth. This is the first demonstration in this model that placental functional compensation is possible and necessary to sustain fetal growth in early HDP. Our data are consistent with other studies in guinea pigs and sheep showing that in late gestation, when fetal nutrient demand is at its greatest and fetal growth is exponential, the compensatory upregulation is no longer sufficient to meet fetal demand [20, 21].

Despite showing increased placental efficiencies in mid-hypertension, we noted no difference in spongiotrophoblast or labyrinth thickness ratios across the mouse gestation. In other words, the trophoblastic and labyrinth layers appear to be proportionally developed in both sham and FGR placentae. This is not surprising because the cell types that form the decidua, junctional zone including the spongiotrophoblast layer, and labyrinth zone are well specified by *E*9.5 in mice and the layered structure of the definitive placenta with thinning of interhemal membrane for efficient exchange is evident by *E*12.5 [22, 23]. Beyond *E*12.5 to full-term gestation, the labyrinth with its fetal vasculature is what continues to expand in size and complexity until delivery [24]. Specifically, the fetal vasculature undergoes secondary branching and elongation and continues to grow in complexity throughout the second half of gestation to produce a large surface area for exchange even though the organization of the labyrinth remains grossly unchanged [25]. Therefore, our reduced CD31 (=PECAM1) staining denoting reduced fetal endothelial cells supports our hypothesis that fetal vascular development is particularly sensitive to gestational hypertension. This defect is different from human HDP in which both shallow invasion and/or failure in trophoblast invasion are believed to be associated with HDP and FGR development [5, 26].

In search for a mechanism for decreased placental labyrinth vascularization, we examined the expression of the hypoxia signaling pathway involving VEGFA and its receptors VEGFR1and VEGFR2 and the MMPs. VEGF-A is one of the potent angiogenic growth factors of the placenta [27]. It not only stimulates vascular growth and permeability, but also promotes vascular endothelial cell protease production and migration, all of which are critical components of

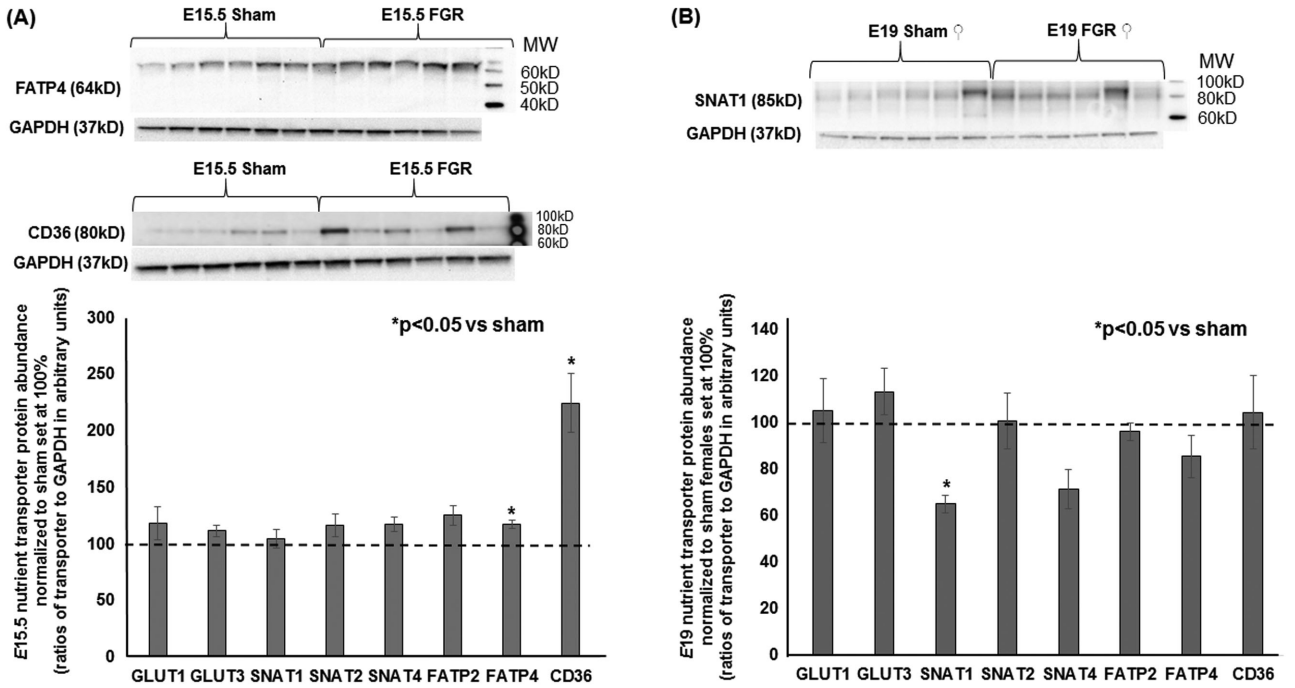

Figure 4. Representative western blots and quantification of placental nutrient transporters at *E*15.5 for sham and TXA_2 analog exposed (FGR) groups and at E19 for sham and FGR females. (A) Quantification of *E*15.5 FGR nutrient transporter abundance of GLUT1, GLUT3, SNAT1, SNAT2, SNAT4, FATP2, FATP4, and CD36 with sham values normalized to 100%. (B) Quantification of *E*19 female FGR nutrient transporter abundance of GLUT1, GLUT3, SNAT1, SNAT2, SNAT4, FATP2, FATP4, and CD36 with sham females normalized to 100%. *Statistical significance declared at $P < 0.05$ for age-matched sham.

the anigogenic process [28]. We found no differences in any of these proteins when comparing FGR males or females to their respective sham males or females. However, we found significant sex differences at baseline between sham offspring and across sexes of the two groups in the expression of many of these proteins. These data demonstrate that sex is a crucial biologic variable in placental studies. Increasing evidence shows that the placenta of one sex over the other might possess different ability to respond and buffer against environmental insults [29]. Animal model and human studies have identified that the placenta expresses select transcripts in a sexually dimorphic manner [30, 31]. If we compared sham males to FGR females, we noted decreased HIF-1α and HIF-2α and increased VHL under a "normal" pregnancy, suggesting that sham males already exhibit decreased hypoxia signaling proteins likely due to increased proteosomal degradation mediated by increased VHL level. The alteration to a FGR pregnancy showed no expected increase in the inducible HIF-1α or HIF-2α to increase hypoxia-mediated signaling genes such as VEGFA. We postulate that other angiogenic factors such as insulin-like growth factor 1 or fibroblast growth factor may play a role in determining vessel growth within the FGR placenta. The roles these factors play in generating our FGR placentae warrant future investigation.

Seeing decreased labyrinth vasculature, we investigated the abundance of important nutrient transporters to better understand the timing and type of compensation that the FGR placentae are capable of. Since glucose is the primary nutrient required for the fetus and placenta, yet the fetus and placenta have a limited ability for producing glucose, we examined two major glucose transporters that transport glucose from the maternal circulation down a concentration gradient to the fetus via facilitated transport with GLUT1 and GLUT3 [32, 33]. In our FGR placentae, we detected no differences in GLUT1 or GLUT3 transporter abundance across the last week of gestation. We interpret this as an adaptation of the FGR placentae such that despite having a reduced vasculature at *E*17.5 and *E*19, glucose transporter expression is maintained to shuttle this important fuel to the fetus. The preserved GLUT1 and GLUT3 abundance would correlate with our previously established fetal glucose levels as being unchanged between sham and FGR pregnancies [10]. Our finding of preserved fetal glucose level is not surprising given that FGR pregnancy has been shown to increase the transplacental glucose gradient and glucose uptake across the placenta [34]. Even though we saw no differences in GLUT1 or GLUT3 expression, we are aware that human studies have shown changes. For example, GLUT3 mRNA expression and protein abundance in the trophoblast on the maternal side of the human placenta was increased in full-term FGR placenta compared with normal placenta [35]. However, in sheep models involving surgical umbilical artery ligation, placental embolism, and uterine carunclectomy, no changes in GLUT transporters were found [36]. The conflicting data present in the literature suggest that the regulation of nutrient transport in FGR pregnancies may depend on the timing and type of insult and be species-specific.

In addition to glucose, other macronutrients are the amino acids and fatty acids. Fetal amino acid concentrations are generally higher than maternal amino acid concentrations, reflecting an active transport system across the placenta [37]. Even though the placenta's role is to supply nutrients to the fetus, it can also produce and utilize amino acids to meet its own metabolic demand, therefore balancing its own need with the fetus' need. One of the major amino acid transporters present in the placenta is the neutral amino acid transporters [38, 39]. System A amino acid transporters are an example of neutral amino acid transporters that facilitate the uptake of small

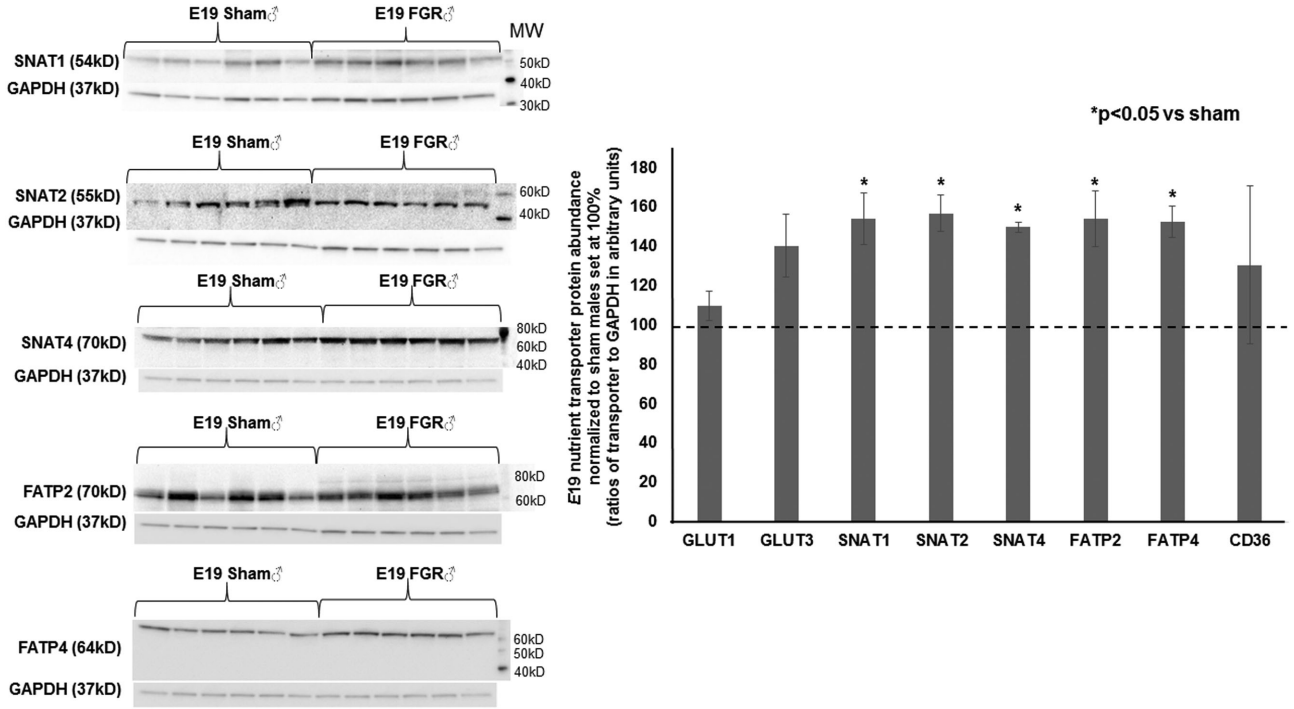

Figure 5. Representative western blots and quantification of placental nutrient transporters at *E*19 for sham and TXA_2 analog exposed (FGR) males. *Statistical significance declared at $P < 0.05$ for age-matched sham males.

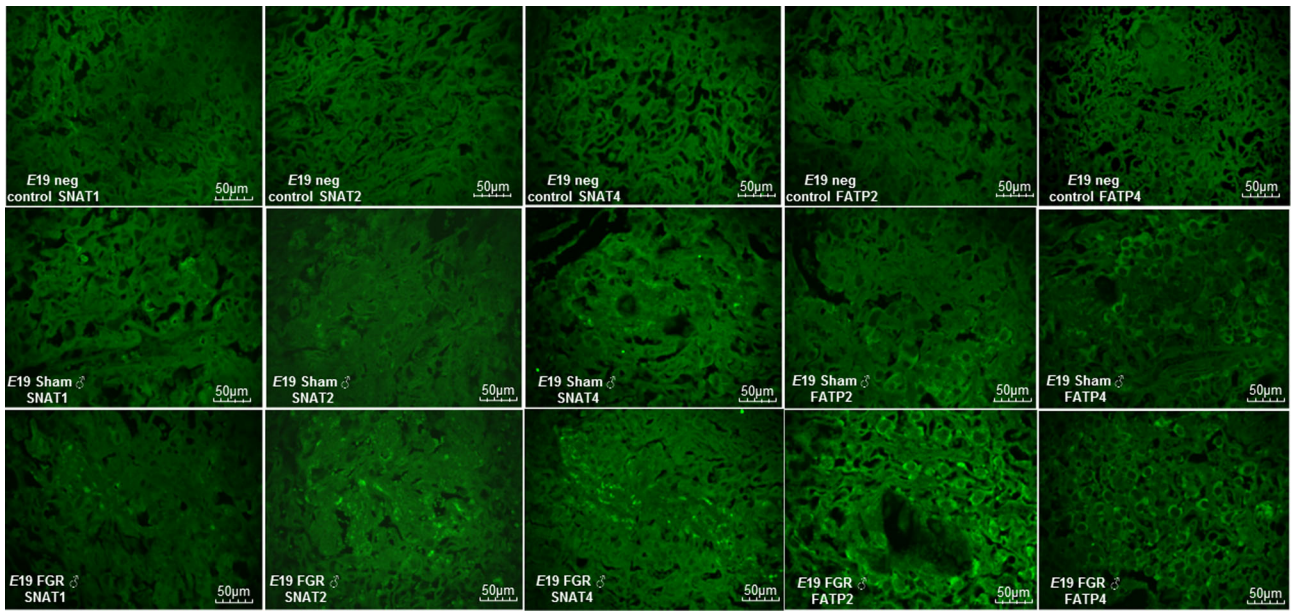

Figure 6. Representative immunofluorescent photomicrographs of *E*19 sham and FGR male placentae of SNAT1, SNAT2, SNAT4, FATP2, and FATP4. The top panels represent negative controls in which the primary antibodies were omitted to denote background fluorescence. The middle panels represent nutrient transporter immunostaining for sham males. The bottom panels represent nutrient transporter immunostaining for FGR males. All immunostaining were obtained at ×40 magnification, and staining can be seen primarily on fetal trophoblasts rather than fetal endothelial cells within the labyrinth layer.

nonessential neutral amino acids such as alanine, glycine, and serine. It also contributes to the high intracellular concentration of glycine which is exchanged for extracellular essential amino acids by system L transporters; therefore, system A transporters are important for the placental transport of both nonessential and essential amino acids [32, 40]. System A consists of three sodium-coupled neutral amino acid transporter (SNAT) proteins, each encoded by independently regulated genes: SNAT1, SNAT2, and SNAT4 [41, 42]. We found intact SNAT abundance in early hypertensive placentae but late hypertensive placentae that support females showed decreased SNAT1. Surprisingly, we detected increased SNATs in late hypertensive placentae supporting males even though fetal growth is

decreased. Explanations for such growth restriction despite increased neutral amino acid transporter in FGR male placentae may be due to the fetus' inability to utilize this substrate for anabolic growth due to inadequate oxygen to drive oxidative metabolism. Alternatively, SNAT localization shows that these transporters are situated in the trophoblasts, most likely in the syncytiotrophoblasts that abutt the fetal endothelial cells; therefore, a lack of vasculature may limit the actual substrate transfer to the fetus. We believe that the inability to utilize amino acids is more consistent with our previously measured fetal serum amino acid levels in which we noted increases in multiple essential (isoleucine, leucine, methionine, phenylalanine, threonine, valine) and nonessential (alanine, hydroxyproline, serine) amino acids in FGR offspring at *E*19.5 [10]. Additionally, these increased amino acid levels are not only a reflection of transporter abundance but also of transporter activity, which we have not measured in this current study. We also have not measured other cationic and anionic amino acid transporters that would contribute to the final fetal amino acid levels. At this juncture, the mechanisms explaining our sex-specific observation remain unknown in this model.

Lastly, fatty acids represent important precursors of bioactive molecules [32]. The primary source of fatty acids taken up by the placenta is maternal TG because their uptake increases significantly in the last trimester [43]. For fatty acids to transfer from the mother to fetus, the cellular membrane FATPs along with fatty acid translocase (FAT/CD36) mediate the cellular uptake of long chain and very long chain fatty acids. We saw increased FATP4 and CD36 expression in early hypertension and increased FATP2 and FATP4 in late hypertensive placentae supporting male fetuses only. Such increased expression may represent compensatory mechanisms to increase fatty acid supply to the fetus. It appears in this model of HDP that placentae supporting male fetuses have a greater capacity for nutrient transfer than those supporting female fetuses, but despite a greater capacity for transfer, its utilization at the fetal level is still limited. It is noteworthy to mention that we have previously shown that male offspring achieve catch-up growth to sham male weights by postnatal day 28 whereas female offspring show a delay until postnatal day 77 [10]. We postulate that the more intact nutrient transfer system in male offspring may partly account for the faster catch-up growth in postnatal life when oxygen needed for metabolism is no longer limited.

We recognize several limitations to our mouse study. First, not one single animal model accurately reflects all pathophysiology of human FGR pregnancies; but because HDP is the most common etiology of placental insufficiency with resultant FGR in the Western world, we have created this model as a tool to answer basic mechanisms of disease that we encounter in clinical medicine. We also acknowledge that there remain differences between human and mouse placentae. An obvious difference is that humans are not litter-bearing animals and the short gestation length in mice compresses the developmental window which may differ from the longer human gestation. Lastly, we have only begun to scratch the surface underlying the mechanisms of placental insufficiency relating to HDP and much work needs to be done to characterize the adaptive and maladaptive responses of the placenta culminating in eventual FGR.

In summary, FGR is an end product of a failed placenta. If our goal is to improve the health of mothers and their children by reducing the incidence of FGR, ongoing investigations aimed at understanding early placental changes during gestation, paying special attention to sex differences, both in animal models and in non-invasive interrogation of human pregnancies, are crucial and necessary steps.

Supplementary data

Supplementary data are available at *BIOLRE* online.

Supplementary Figure S1. Representative western blots of hypoxia signaling proteins at *E*19 for sham and TXA_2 analog exposed (FGR) placentae. (A) Western immunoblots of *E*19 HIF-1α, HIF-2α, HIF-1β, PHD2, VHL, and VEGFA abundance for FGR and sham female placentae. α-Tubulin was used as a loading control which was measured to be unchanged between sham and FGR. (B) Western immunoblots of *E*19 HIF-1α, HIF-2α, HIF-1β, PHD2, VHL, and VEGFA abundance for FGR and sham male placentae. α-Tubulin was used as a loading control which was measured to be unchanged between sham and FGR.

Supplementary Figure S2. Representative western blots of matrix metalloproteins at *E*19 for sham and TXA_2 analog exposed (FGR) placentae. (A) Western immunoblots of *E*19 MMP2, MMP9, MMP14, MMP15, MMP16, MMP 17, MMP24, MMP25, CD147 abundance for FGR and sham female placentae. α-Tubulin was used as a loading control which was measured to be unchanged between sham and FGR. (B) Western immunoblots of *E*19 MMP2, MMP9, MMP14, MMP15, MMP16, MMP 17, MMP24, MMP25, CD147 abundance for FGR and sham male placentae. α-Tubulin was used as a loading control which was measured to be unchanged between sham and FGR.

Supplementary Table S1. Antibodies used in this study including antibody names, product ID numbers, research resource IDs, and commercial companies that supply the antibodies.

References

1. Maulik D. Fetal growth restriction: the etiology. *Clin Obstet Gynecol* 2006; **49**:228–235.
2. Salafia CM, Minior VK, Pezzullo JC, Popek EJ, Rosenkrantz TS, Vintzileos AM. Intrauterine growth restriction in infants of less than thirty-two weeks' gestation: associated placental pathologic features. *Am J Obstet Gynecol* 1995; **173**:1049–1057.
3. Froen JF, Gardosi JO, Thurmann A, Francis A, Stray-Pedersen B. Restricted fetal growth in sudden intrauterine unexplained death. *Acta Obstet Gynecol Scand* 2004; **83**:801–807.
4. Lockwood CJ, Huang SJ, Krikun G, Caze R, Rahman M, Buchwalder LF, Schatz F. Decidual hemostasis, inflammation, and angiogenesis in preeclampsia. *Semin Thromb Hemost* 2011; **37**:158–164.
5. Lyall F, Robson SC, Bulmer JN. Spiral artery remodeling and trophoblast invasion in preeclampsia and fetal growth restriction: relationship to clinical outcome. *Hypertension* 2013; **62**:1046–1054.
6. Roberts DJ, Post MD. The placenta in pre-eclampsia and intrauterine growth restriction. *J Clin Pathol* 2008; **61**:1254–1260.
7. Soto E, Romero R, Kusanovic JP, Ogge G, Hussein Y, Yeo L, Hassan SS, Kim CJ, Chaiworapongsa T. Late-onset preeclampsia is associated with an imbalance of angiogenic and anti-angiogenic factors in patients with and without placental lesions consistent with maternal underperfusion. *J Matern Fetal Neonatal Med* 2012; **25**: 498–507.
8. Kovo M, Schreiber L, Ben-Haroush A, Gold E, Golan A, Bar J. The placental component in early-onset and late-onset preeclampsia in relation to fetal growth restriction. *Prenat Diagn* 2012; **32**:632–637.
9. Nelson DB, Ziadie MS, McIntire DD, Rogers BB, Leveno KJ. Placental pathology suggesting that preeclampsia is more than one disease. *Am J Obstet Gynecol* 2014; **210**:66 e61-67.
10. Fung C, Brown A, Cox J, Callaway C, McKnight R, Lane R. Novel thromboxane A_2 analog-induced IUGR mouse model. *J Devel Orig Health Dis* 2011; **2**:291–301.
11. Fung CM, Yang Y, Fu Q, Brown AS, Yu B, Callaway CW, Li J, Lane RH, McKnight RA. IUGR prevents IGF-1 upregulation in juvenile male mice

by perturbing postnatal IGF-1 chromatin remodeling. *Pediatr Res* 2015; **78**:14–23.
12. Fung CM, White JR, Brown AS, Gong H, Weitkamp JH, Frey MR, McElroy SJ. Intrauterine growth restriction alters mouse intestinal architecture during development. *PLoS ONE* 2016; **11**:e0146542.
13. Croy A, Yamada AT, DeMayo FJ, Adamson SL. *The Guide to Investigation of Mouse Pregnancy*. London, UK: Elsevier; 2014: 143–161.
14. Dilworth MR, Sibley CP. Review: Transport across the placenta of mice and women. *Placenta* 2013; **34** Suppl:S34–S39.
15. Bowen RS, Zhang Y, Gu Y, Lewis DF, Wang Y. Increased phospholipase A2 and thromboxane but not prostacyclin production by placental trophoblast cells from normal and preeclamptic pregnancies cultured under hypoxia condition. *Placenta* 2005; **26**:402–409.
16. Shah DA, Khalil RA. Bioactive factors in uteroplacental and systemic circulation link placental ischemia to generalized vascular dysfunction in hypertensive pregnancy and preeclampsia. *Biochem Pharmacol* 2015; **95**:211–226.
17. Harding JE, Johnston BM. Nutrition and fetal growth. *Reprod Fertil Dev* 1995; **7**:539–547.
18. Sibley C, Glazier J, D'Souza S. Placental transporter activity and expression in relation to fetal growth. *Exp Physiol* 1997; **82**:389–402.
19. Angiolini E, Fowden A, Coan P, Sandovici I, Smith P, Dean W, Burton G, Tycko B, Reik W, Sibley C, Constancia M. Regulation of placental efficiency for nutrient transport by imprinted genes. *Placenta* 2006; **27** Suppl A:98–102.
20. Soo PS, Hiscock J, Botting KJ, Roberts CT, Davey AK, Morrison JL. Maternal undernutrition reduces P-glycoprotein in guinea pig placenta and developing brain in late gestation. *Reprod Toxicol* 2012; **33**:374–381.
21. Robinson JS, Kingston EJ, Jones CT, Thorburn GD. Studies on experimental growth retardation in sheep. The effect of removal of a endometrial caruncles on fetal size and metabolism. *J Dev Physiol* 1979; **1**:379–398.
22. Riley P, Anson-Cartwright L, Cross JC. The Hand1 bHLH transcription factor is essential for placentation and cardiac morphogenesis. *Nat Genet* 1998; **18**:271–275.
23. Scott IC, Anson-Cartwright L, Riley P, Reda D, Cross JC. The HAND1 basic helix-loop-helix transcription factor regulates trophoblast differentiation via multiple mechanisms. *Mol Cell Biol* 2000; **20**:530–541.
24. Simmons DG, Natale DR, Begay V, Hughes M, Leutz A, Cross JC. Early patterning of the chorion leads to the trilaminar trophoblast cell structure in the placental labyrinth. *Development* 2008; **135**:2083–2091.
25. Coan PM, Ferguson-Smith AC, Burton GJ. Developmental dynamics of the definitive mouse placenta assessed by stereology. *Biol Reprod* 2004; **70**:1806–1813.
26. Kaufmann P, Black S, Huppertz B. Endovascular trophoblast invasion: implications for the pathogenesis of intrauterine growth retardation and preeclampsia. *Biol Reprod* 2003; **69**:1–7.
27. Klagsbrun M. Regulators of angiogenesis: stimulators, inhibitors, and extracellular matrix. *J Cell Biochem* 1991; **47**:199–200.
28. Folkman J, Klagsbrun M. Angiogenic factors. *Science* 1987; **235**: 442–447.
29. Rosenfeld CS. Sex-specific placental responses in fetal development. *Endocrinology* 2015; **156**:3422–3434.
30. Steier JA, Bergsjo PB, Thorsen T, Myking OL. Human chorionic gonadotropin in maternal serum in relation to fetal gender and utero-placental blood flow. *Acta Obstet Gynecol Scand* 2004; **83**: 170–174.
31. Brown ZA, Schalekamp-Timmermans S, Tiemeier HW, Hofman A, Jaddoe VW, Steegers EA. Fetal sex specific differences in human placentation: a prospective cohort study. *Placenta* 2014; **35**:359–364.
32. Lager S, Powell TL. Regulation of nutrient transport across the placenta. *J Pregnancy* 2012; **2012**:1–14.
33. Brown K, Heller DS, Zamudio S, Illsley NP. Glucose transporter 3 (GLUT3) protein expression in human placenta across gestation. *Placenta* 2011; **32**:1041–1049.
34. Marconi AM, Paolini CL. Nutrient transport across the intrauterine growth-restricted placenta. *Semin Perinatol* 2008; **32**:178–181.
35. Janzen C, Lei MY, Cho J, Sullivan P, Shin BC, Devaskar SU. Placental glucose transporter 3 (GLUT3) is up-regulated in human pregnancies complicated by late-onset intrauterine growth restriction. *Placenta* 2013; **34**:1072–1078.
36. Zhang S, Regnault TR, Barker PL, Botting KJ, McMillen IC, McMillan CM, Roberts CT, Morrison JL. Placental adaptations in growth restriction. *Nutrients* 2015; **7**:360–389.
37. Regnault TR, Friedman JE, Wilkening RB, Anthony RV, Hay WW, Jr. Fetoplacental transport and utilization of amino acids in IUGR — a review. *Placenta* 2005; **26** (Suppl A):S52–S62.
38. Grillo MA, Lanza A, Colombatto S. Transport of amino acids through the placenta and their role. *Amino Acids* 2008; **34**:517–523.
39. Desforges M, Sibley CP. Placental nutrient supply and fetal growth. *Int J Dev Biol* 2010; **54**:377–390.
40. Jones HN, Powell TL, Jansson T. Regulation of placental nutrient transport–a review. *Placenta* 2007; **28**:763–774.
41. Constancia M, Angiolini E, Sandovici I, Smith P, Smith R, Kelsey G, Dean W, Ferguson-Smith A, Sibley CP, Reik W, Fowden A. Adaptation of nutrient supply to fetal demand in the mouse involves interaction between the Igf2 gene and placental transporter systems. *Proc Natl Acad Sci USA* 2005; **102**:19219–19224.
42. Desforges M, Greenwood SL, Glazier JD, Westwood M, Sibley CP. The contribution of SNAT1 to system A amino acid transporter activity in human placental trophoblast. *Biochem Biophys Res Commun* 2010; **398**:130–134.
43. Haggarty P. Fatty acid supply to the human fetus. *Annu Rev Nutr* 2010; **30**:237–255.